428 *J. Chem. Eng. Data* 1991, *36*, 428-430

Excess Enthalpies of α,ω-Dibromoalkane + *n*-Hexane Mixtures at 298.15 K and Isothermal Vapor–Liquid Equilibrium of 1,3-Dibromopropane + *n*-Nonane at 348.15 K

José Muñoz Embid, Manuela Artal, Javier Fernández, Inmaculada Velasco, and Santos Otín*

Departamento de Química Orgánica-Química Física, Facultad de Ciencias, Universidad de Zaragoza, 50009-Zaragoza, Spain

Excess enthalpies at 298.15 K have been measured for liquid *n*-hexane + 1,3-dibromopropane, + 1,4-dibromobutane, + 1,5-dibromopentane, + 1,6-dibromohexane, or + 1,8-dibromooctane mixtures. Moreover, isothermal vapor–liquid equilibrium has been obtained for 1,3-dibromopropane + *n*-nonane at 348.15 K, and the excess Gibbs energy was derived.

Introduction

Following our systematic study of the thermodynamic properties of binary liquid mixtures containing haloalkanes (*1–5*), we present here the molar excess enthalpies H^E at 298.15 K of five binary α,ω-dibromoalkane + *n*-hexane mixtures. As far as we know, the only previous measurements on this type of mixtures are those of 1,2-dibromoethane in several *n*-alkanes (*6–8*). Moreover, we have measured the vapor–liquid equilibrium (VLE) of 1,3-dibromopropane + *n*-nonane, at 348.15 K.

Experimental Section

Materials. All the chemicals were from Fluka. 1,3-Dibromopropane was "purum" product, with stated minimum purity of 99%; 1,4-dibromobutane, 1,5-dibromopentane, and 1,8-dibromooctane were "purum" products with stated minimum purities of 98%, and 1,6-dibromohexane was a "pract." product with stated purity of ca. 97%; *n*-hexane was a "puriss p.a." product and *n*-nonane was a "purum" product with stated minimum purities of 99%.

In Table I we compare the measured densities, refractive indexes, and vapor pressures of the products with literature values.

Apparatus and Procedure. Vapor–liquid equilibrium data were taken at constant temperature in a dynamic still designed by Berro et al. (*9*). The temperature T inside the equilibrium cell was measured with a precision of 0.01 K by means of a Digitec digital thermometer (Digitec Corp.) Model 5831. The pressure was measured by means of a Digiquartz Transmitter of Paroscientific Inc., Model 1015A, calibrated in the pressure range 0–0.1 MPa. The accuracy of the pressure measurements is 0.01%. Liquid and vapor mole fractions x_i and y_i, respectively, were determined by densimeter analysis using an Anton Paar Model DMA 60 densimeter equipped with a DMA 602 cell. The densimeter was coupled to the ebulliometer and operated with continuous circulation of the equilibrium liquid and condensed vapor through the densimeter cell. The streams were circulated by means of a peristaltic pump (Gilson; HP2), with low, constant flow, and a rotary valve permitting the selection of either the liquid or condensed vapor to pass through the densimeter cell (Figure 1). After passing through the densimeter, both streams were recirculated to the ebulliometer. Teflon tubes were used for the connections. The elastic segments of the tubes passing through the peristaltic pumps were made from solvent-resistant elastomer (isoversinic). The total volume of liquid outside the ebulliometer (i.e., circulating through the analysis system) was ca. 5 mL, which is ca. 6% of the total material contained in the ebulliometer. The flow through the densimeter was sufficiently low to ensure the stability of temperature in the measuring cell. We verified that the circulating system functioned properly over the range of pressures normally used for ebulliometric measurements. The temperature in the cell was measured with an Anton Paar DT100-30 digital thermometer, with a precision of 0.01 K. The densities were previously determined to better than 0.000 02 g cm^{-3} in the same densimeter. Binary mixtures were prepared by weighing.

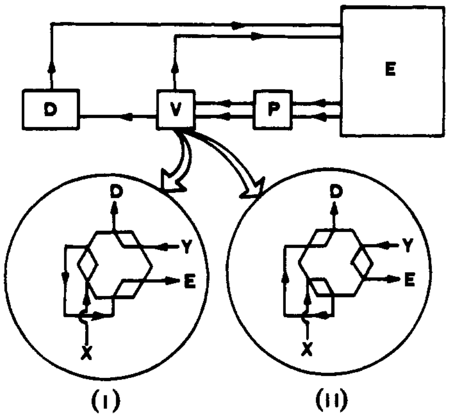

Figure 1. Flow diagram for sampling and determination of liquid- and vapor-phase compositions: E, ebulliometer; P, peristaltic pump; D, densimeter; V, rotary valve; (I), analysis of vapor phase (Y); (II), analysis of liquid phase (X).

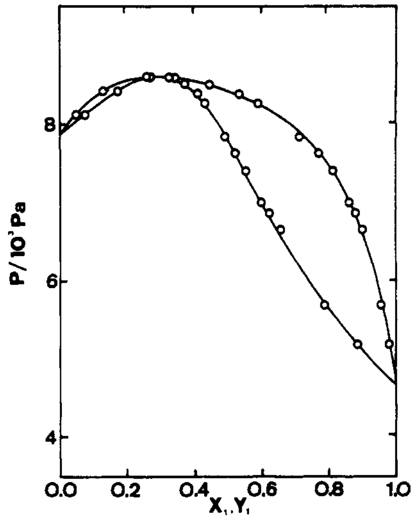

Figure 2. Vapor–liquid equilibrium diagram at 348.15 K: pressure, P, as a function of mole fraction in liquid, x_1, or vapor, y_1, phase for 1,3-dibromopropane (1) + *n*-nonane (2): Continuous curves, smoothed values; points, direct experimental values.

0021-9568/91/1736-0428\$02.50/0 © 1991 American Chemical Society

Table I. Densities $\rho_i°$, Refractive Indexes n_D, and Vapor Pressures $P_i°$ of the Pure Components at Temperature T

	T/K	$\rho_i°/(g\ cm^{-3})$ this work	$\rho_i°/(g\ cm^{-3})$ lit.[a]	n_D this work	n_D lit.[a]	$P_i°/(10^3\ Pa)$ this work	$P_i°/(10^3\ Pa)$ lit.
1,3-dibromopropane	298.15	1.971 18	1.971 3	1.520 42	1.520 8		
	348.15					4.672	4.706[b] 4.661[c]
1,4-dibromobutane	298.15	1.816 77	1.818 7	1.516 18	1.516 9		
1,5-dibromopentane	298.15	1.699 55	1.694 8	1.510 64	1.510 3		
1,6-dibromohexane	298.15	1.599 43	1.504 96				
1,8-dibromooctane	298.15	1.457 91	1.498 00				
n-hexane	298.15	0.654 60	0.654 84	1.369 94	1.372 26		
n-nonane	298.15	0.713 85	0.713 75	1.403 10	1.403 11		
	348.15					7.854	7.853[a]

[a] Reference 16. [b] Reference 17. [c] Reference 18.

Table II. Excess Molar Enthalpies H^E at 298.15 K as a Function of Mole Fraction x_1, Coefficients A_j (Equation 1), and Standard Deviations $\sigma(H^E)$ (Equation 3)

1,3-Dibromopropane (1) + *n*-Hexane (2)

x_1	H^E/(J mol^{-1})	x_1	H^E/(J mol^{-1})	x_1	H^E/(J mol^{-1})
0.0508	286	0.3613	1271	0.7872	884
0.1036	542	0.4123	1320	0.8333	726
0.1211	618	0.4514	1344	0.8904	522
0.1791	827	0.5239	1326	0.9411	305
0.2660	1080	0.6262	1242		
0.3100	1181	0.6961	1113		

$$H^E/x_1(1-x_1)\ J\ mol^{-1} = 5363 - 318(2x_1-1) + 290(2x_1-1)^2$$
$$\sigma(H^E)/(J\ mol^{-1}) = 6.9$$

1,4-Dibromobutane (1) + *n*-Hexane (2)

x_1	H^E/(J mol^{-1})	x_1	H^E/(J mol^{-1})	x_1	H^E/(J mol^{-1})
0.0825	473	0.4013	1278	0.7403	971
0.1047	570	0.5000	1293	0.8094	765
0.2101	940	0.5807	1257	0.8970	457
0.2992	1152	0.6919	1088		

$$H^E/x_1(1-x_1)\ J\ mol^{-1} = 5202 - 401(2x_1-1) + 467(2x_1-1)^2 - 562(2x_1-1)^3$$
$$\sigma(H^E)/(J\ mol^{-1}) = 5.8$$

1,5-Dibromopentane (1) + *n*-Hexane (2)

x_1	H^E/(J mol^{-1})	x_1	H^E/(J mol^{-1})	x_1	H^E/(J mol^{-1})
0.1020	534	0.3926	1197	0.7957	746
0.2023	881	0.4747	1195	0.8494	570
0.2944	1097	0.5683	1146		
0.3424	1154	0.6692	1022		

$$H^E/x_1(1-x_1)\ J\ mol^{-1} = 4793 - 817(2x_1-1) + 633(2x_1-1)^2$$
$$\sigma(H^E)/(J\ mol^{-1}) = 8.8$$

1,6-Dibromohexane (1) + *n*-Hexane (2)

x_1	H^E/(J mol^{-1})	x_1	H^E/(J mol^{-1})	x_1	H^E/(J mol^{-1})
0.0668	377	0.5000	1055	0.8018	598
0.2161	809	0.5754	995	0.9040	329
0.3088	955	0.6830	849		

$$H^E/x_1(1-x_1)\ J\ mol^{-1} = 4201 - 631(2x_1-1) - 359(2x_1-1)^2 - 812(2x_1-1)^3 + 1823(2x_1-1)^4$$
$$\sigma(H^E)/(J\ mol^{-1}) = 4.6$$

1,8-Dibromooctane (1) + *n*-Hexane (2)

x_1	H^E/(J mol^{-1})	x_1	H^E/(J mol^{-1})	x_1	H^E/(J mol^{-1})
0.0577	208	0.3491	854	0.6931	640
0.1010	355	0.3967	867	0.7743	502
0.1481	508	0.4698	855	0.8839	294
0.2034	639	0.5574	815		
0.2922	796	0.6061	751		

$$H^E/x_1(1-x_1)\ J\ mol^{-1} = 3392 - 1177(2x_1-1) + 186(2x_1-1)^2 + 760(2x_1-1)^3 - 299(2x_1-1)^4$$
$$\sigma(H^E)/(J\ mol^{-1}) = 6.2$$

Molar excess enthalpies H^E were determined by using isobaric and quasi-isothermic calorimeter similar to that described in ref 10. Electrical energy was measured to better than 0.5%. The temperature in the water bath was controlled to within 0.002 K. The estimated errors are $\sigma_e(x_i) < 0.0002$ and $\sigma_e(T) = 0.01$ K (*11*). The calorimeter was checked against *n*-hexane + cyclohexane, at 298.15 K, the agreement with the data of ref 12 being better than 0.5% over the central range of concentration.

Table III. Experimental Vapor–Liquid Equilibrium Pressure P and Vapor Mole Fraction y_1 at 348.15 K as a Function of Liquid Mole Fraction x_1, Coefficients A_j (Equation 2), Standard Deviations $\sigma(P)$ and $\sigma(y_1)$ (Equation 3), Molar Second Virial Coefficients B_{ij}, and Liquid Molar Volumes of Pure Components $V_i°$

x_1	y_1	$P/(10^3\ Pa)$	x_1	y_1	$P/(10^3\ Pa)$
0.0503	0.0744	8.119	0.7695	0.5211	7.630
0.1298	0.1740	8.419	0.8111	0.5520	7.405
0.2603	0.2744	8.600	0.8621	0.5987	6.996
0.3460	0.3253	8.594	0.8804	0.6217	6.859
0.4462	0.3728	8.513	0.9005	0.6563	6.651
0.5336	0.4092	8.391	0.9551	0.7871	5.693
0.5898	0.4319	8.269	0.9800	0.8849	5.188
0.7124	0.4905	7.840			

$$G^E/x_1(1-x_1)RT\ J\ mol^{-1} = 1.21678 + 0.15151(2x_1-1) + 0.08635(2x_1-1)^2$$
$$\sigma(P)/(10^3\ Pa) = 0.028;\ \sigma(y_1) = 0.0046$$
$$B_{11}/(cm^3\ mol^{-1}) = -2735;\ B_{22}/(cm^3\ mol^{-1}) = -3640$$
$$B_{12}/(cm^3\ mol^{-1}) = -2596$$
$$V_1°/(cm^3\ mol^{-1}) = 107;\ V_2°/(cm^3\ mol^{-1}) = 190$$

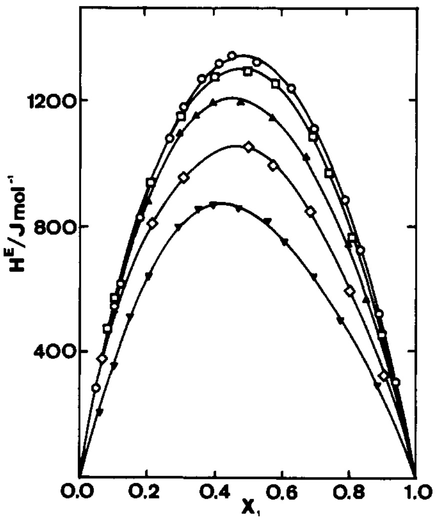

Figure 3. Excess molar enthalpies H^E at 298.15 K as a function of mole fraction x_1. Continuous curves, smoothed values, eq 1; points, direct experimental values; (○) 1,3-dibromopropane (1), or (□) 1,4-dibromobutane (1), or (△) 1,5-dibromopentane (1), or (◇) 1,6-dibromohexane (1), or (▽) 1,8-dibromooctane (1) + *n*-hexane (2).

Results and Discussion

Molar excess Gibbs energies G^E were calculated by reduction of the experimental P–x_1 data with the Redlich–Kister equation. Vapor-phase nonideality and the variation of the Gibbs energy of the pure liquid components with pressure were accounted for in terms of the molar second virial coefficients B_{ij}, estimated by the method of Tsonopoulos (*13*, *14*) and the liquid molar volumes $V_i°$. The critical constants for 1,3-dibromopropane (T_c = 669 K, P_c = 5414 kPa) were estimated by the Joback method (modification of Lydersen's method) (*15*).

The H^E values at 298.15 K and G^E values at 348.15 K are collected in Tables II and III. Smoothing equations of the type

$$H^E_{calc}/x_1(1 - x_1) = \sum A_j(2x_1 - 1)^{j-1} \tag{1}$$

and

$$G^E_{calc}/x_1(1 - x_1)RT = \sum A_j(2x_1 - 1)^{j-1} \tag{2}$$

were fitted by the method of least-squares.

The A_j parameters are given in Tables II and III together with the standard deviations $\sigma(Q)$ calculated as

$$\sigma(Q) = [\sum(Q - Q_{calc})^2/N]^{1/2} \tag{3}$$

where N is the number of experimental values and $Q = H^E$, P, or y_1.

For 1,3-dibromopropane + n-nonane (Figure 2), formation of a maximum-boiling azeotrope was observed ($x_{1,Az} = 0.2926$, $P_{Az} = 8603$ Pa).

The H^E values are all positive (Figure 3) and decrease with increasing separation of the bromine atoms in the molecule. At the same time, the maxima of the H^E–x curves shift gradually toward the α,ω-dibromo-rich side. A general discussion of these results is deferred until other mixtures containing polybromoalkanes are investigated.

Glossary

A_j	parameters in eq 1 or 2
B_{ij}	molar second virial coefficients, cm^3 mol^{-1}
G	molar Gibbs energy, J mol^{-1}
H	molar enthalpy, J mol^{-1}
N	total number of measurements
P	total vapor pressure, Pa
Q	any property
R	molar gas constant (8.314 51 J K^{-1} mol^{-1})
T	temperature, K
V	liquid molar volume, cm^3 mol^{-1}
x	liquid mole fraction
y	vapor mole fraction

Greek Letters

$\sigma(Q)$	standard deviation of property Q, eq 3
σ_e	experimental uncertainty

Superscripts

E	excess property
o	pure component

Subscripts

Az	azeotropic property
calc	calculated property
i	type of component

Registry No. n-Hexane, 110-54-3; 1,4-dibromobutane, 110-52-1; 1,5-dibromopentane, 111-24-0; 1,6-dibromohexane, 629-03-8; 1,8-dibromooctane, 4549-32-0; 1,3-dibromopropane, 109-64-8; nonane, 111-84-2.

Literature Cited

(1) Muñoz Embid, J.; Velasco, I.; Otín, S.; Gutierrez Losa, C.; Kehiaian, H. V. *Fluid Phase Equilib*. **1987**, *38*, 1.
(2) García-Lisbona, N.; García Vicente, I.; Muñoz Embid, J.; Velasco, I.; Otín, S.; Kehiaian, H. V. *Fluid Phase Equilib*. **1989**, *45*, 191.
(3) Soriano, M. J.; Velasco, I.; Otín, S.; Kehiaian, H. V. *Fluid Phase Equilib*. **1989**, *45*, 205.
(4) Muñoz Embid, J.; Berro, C.; Otín, S.; Kehiaian, H. V. *J. Chem. Eng. Data* **1990**, *35*, 266.
(5) Artal, M.; Fernández, J.; Muñoz Embid, J.; Velasco, I.; Otín, S.; Kehiaian, H. V. *J. Solution Chem*. **1991**, *20*, 1.
(6) Morón, M. C.; Pérez, P.; Gracia, M.; Gutiérrez Losa, C. *J. Chem. Thermodyn*. **1985**, *17*, 733.
(7) Delmas, G.; Purves, P. *J. Chem. Soc., Faraday Trans. 2* **1977**, *73*, 1828.
(8) Delmas, G.; Purves, P. *J. Chem. Soc., Faraday Trans. 2* **1977**, *73*, 1838.
(9) Berro, C.; Rogalski, M.; Péneloux, A. *Fluid Phase Equilib*. **1982**, *8*, 55.
(10) Gutiérrez Losa, C.; Gracia, M. *Rev. Acad. Cienc. Exactas, Fis., Quím. Nat. Zaragoza* **1971**, *26*, 101.
(11) Velasco, I.; Otín, S.; Gutiérrez Losa, C. *Int. DATA Ser., Sel. Data Mixtures, Ser. A* **1979**, 8.
(12) Marsh, K. N. *Int. DATA Ser., Sel. Data Mixtures, Ser. A* **1973**, 22.
(13) Tsonopoulos, C. *AIChE J*. **1974**, *20*, 263.
(14) Tsonopoulos, C. *AIChE J*. **1975**, *21*, 827.
(15) Reid, R. C.; Prausnitz, J. M.; Poling, B. E. *The Properties of Gases and Liquids*, McGraw-Hill: New York, 1986.
(16) TRC Thermodynamic Tables; Thermodynamics Research Center, The Texas A&M University System: College Station, TX.
(17) Stull, D. R. *Ind. Eng. Chem*. **1947**, *39*, 517. Cf.: Ohe, S. *Computer Aided Data Book of Vapor Pressure*; Data Book Publishing Co.: Tokyo, 1976.
(18) Dykyj, J.; Repáš, M.; Svoboda, J. *Tlak nasytenej pary organickych zlucenin (pokracovanie)*; Vydavatel'stvo Slovenskej Akadémie Vied: Bratislava, 1984.

Received for review February 25, 1991. Revised June 14, 1991. Accepted July 22, 1991. We gratefully acknowledge the financial support received from Dirección General de Investigación Científica y Técnica de España (Proyecto PB 86-0184).

Solubilities of Myristic Acid, Palmitic Acid, and Cetyl Alcohol in Supercritical Carbon Dioxide at 35 °C

Yoshio Iwai,* Takao Fukuda, Yoshio Koga, and Yasuhiko Arai

Department of Chemical Engineering, Faculty of Engineering, Kyushu University, Fukuoka 812, Japan

A flow-type apparatus was constructed to measure the solubilities of myristic acid (tetradecanoic acid), palmitic acid (hexadecanoic acid), and cetyl alcohol (hexadecanol) in supercritical carbon dioxide at 35 °C from 8.1 to 22.8, 9.9 to 20.6, and 8.9 to 21.8 MPa, respectively. The logorithm of the enhancement factor was plotted against the density of carbon dioxide, and a good linear relationship was observed for each system.

Introduction

It is very useful if natural products can be separated and purified with high selectivity. The supercritical gas extraction has been given much attention recently as one of the new separation technologies in the chemical industry. The solubility data of natural products in supercritical gas are essentially important in the process design of the supercritical gas extraction. In this work, a flow-type apparatus was constructed to measure the solubilities of myristic acid, palmitic acid, and